Advances in Engineering Software 179 (2023) 103434

Contents lists available at ScienceDirect

Advances in Engineering Software

journal homepage: www.elsevier.com/locate/advengsoft

Stochastic analysis of steel frames considering the material, geometrical and loading uncertainties

Huy-Khanh Dang, Duc-Kien Thai, Seung-Eock Kim *

Department of Civil and Environmental Engineering, Sejong University, 98 Gunja Dong, Gwangjin Gu, Seoul, 05006, South Korea

ARTICLE INFO

Keywords:
Stochastic analysis
Statistic approach
Steel structure
Bayesian model averaging
Monte carlo sampling
Latin hypercube sampling
Reliability
Sensitivity

ABSTRACT

This paper develops a Stochastic Practical Advanced Analysis Program for stochastic analysis of structural steel frames. The second-order refined plastic-hinge analysis method combined with the technical simulation of Latin Hypercube Sampling is developed to predict the actual ultimate load-carrying capacity of steel frames and investigate the sensitivity of the uncertain input parameters. The input parameters of material properties, geometrical characteristics, and load combinations are considered as independent random variables that may occur in simultaneous randomness. A proposed parallel analytical technique integrates the modified Newton-Raphson and Generalized Displacement Control algorithms to solve the nonlinear inelastic problems to estimate the critical displacement-based system reliability index. The results of the statistical analysis in terms of coefficients of variation and Pearson correlation index show that the yield strength of material is the most sensitive with respect to the behavior of steel frames. The Bayesian Model Averaging is employed to find the most influential structural components on the ultimate structural resistance. The useful results of this research may be used in steel structure design and maintenance in practice.

1. Introduction

Steel structures have been widely used in construction, especially for industrial or tall buildings [1,2]. Numerous researchers have focused on identifying the most precise methods or surrogate models for evaluating the responsiveness of the structure in various conditions under static, extreme and seismic loads [3–9] and finding solution to optimize the steel structures [10–12]. There are numerous applicable calculation tools capable of dealing with the distinct types of steel frames, some of which are based on the finite element method (FEM). This method offers a high degree of intuitiveness and accuracy, is widely applicable, but requires a great deal of time and processing resources [13]. It is frequently used as a benchmark to compare and develop other methods that are more time- and computing-efficient. One of these is the elastic-plastic analysis approach, which has just been extensively explored and developed for steel frame problems. This method can be divided into two primary categories: 1) Plastic zone (distributed plasticity) and 2) Plastic hinge (Concentrated plastic hinge). The plastic zone approach is regarded as the proper way since it is easy to account for advanced effects in steel structures, such as gradual spread yielding, residual stress, geometric imperfection, and material strain hardening [14–17]. However, due to its complexity and expense [18], this type of study is too computationally intensive for application in general design. In reality, when a steel frame subjected to an ultimate load, the inelastic behavior occurs on the plastic joints, while other portions of the member continue to function within the elasticity. In order to replace the conventional elastic-plastic hinge analysis method, a second-order refined plastic hinge analysis method has been developed that takes into consideration the advanced effects similar to the plastic zone method [19–22]. In comparison to the plastic zone method and the FEM [23,24], the refined plastic hinge method yields enough reliability. In addition, this method uses just one beam-column element per member, making it significantly more efficient and cost-effective than the plastic zone approach, therefore, it is used in this investigation.

The problem of the steel structure frame calculation model has, thus, gained enough dependability to find the accurate behavior of the structure, reducing considerable epistemic uncertainty [25]. Nonetheless, numerous uncertainties in loads, geometry, and material properties occur in practical engineering systems [26–28], which are referred to as aleatory uncertainty, whereas in traditional deterministic analysis, the uncertainty quantification and the structural propagation are not addressed. As a result, the structure uses standard deterministic

* Corresponding author.
E-mail address: sekim@sejong.ac.kr (S.-E. Kim).

https://doi.org/10.1016/j.advengsoft.2023.103434
Received 23 September 2022; Received in revised form 26 January 2023; Accepted 9 February 2023
Available online 18 February 2023

methodologies that may face failure risks in an uncertain environment. Developing computer approaches for structural analysis and design accounting for random uncertainty has emerged as an important research area [29–34]. Among the several approaches for analyzing issues with random parameters [35–37], the stochastic finite element method (SFEM) [38] has been developed and applied to the assessment of dependability and response variability in static and dynamic, linear, and non-linear situations. Papadrakakis et al. [39] have devised a novel parallel computer implementation methodologies in conjunction with the Monte Carlo Simulation and the weighted integral method to create efficient numerical processing of SFEM. Wang et al. [40] created an extended polynomial chaos expansion that takes into consideration both aleatory and epistemic uncertainty. The perturbation approach is used to estimate the mean and variance of the response [41]. These methods are approximate since the series expansion must be shortened after a few terms. Each term in the series represents the response of the same deterministic system to various effective random forcing functions. In this research, we address aleatory uncertainty as random variables in the accurate evaluation of steel structural response using the Monte Carlo simulation (MCS) in conjunction with a refined plastic hinge analysis approach and supplement the evaluation of system reliability and sensitivity of input parameters. Our approach can be used to supplement conventional deterministic analysis, moreover, accounting for stochastic system behaviors, therefore, the failure probability of structures can be significantly reduced. In general, the type of uncertainty dispersed in a continuum structure is characterized as random fields, where the value at each point is a random variable and various correlating points.

The study is conducted on a complex steel structure with many components. For each component, input parameters are treated as random variables. Thus, every random combination of input variable for the steel frame will yield a random structural scenario subjected to a random combination of loads, which is entirely feasible in the actual world. The Practical Advanced Analysis Program (PAAP) estimates each stochastic situation's ultimate resistance state. Probability distributions of result sets produce quantities of interest to determine the accurate steel frame's load-carrying capacity, the system's reliability, and the impact of each input variable. In order to reduce computational costs, we must compute the minimal number of input variable samples needed to provide adequate outputs. Thus, the Latin Hypercube Sampling (LHS) strategy can generate enough random samples for statistically significant analysis [42]. The stochastic analysis shows that uncertainty in input parameters lowers the structure's load-carrying capability compared to deterministic analysis. Steel yield strength is very sensitive to the frame's load capacity. Parallel analytic techniques of nonlinear modified Newton-Raphson (mNR) and General Displacement Control (GDC) algorithms can evaluate a structural system's failure probability and reliability index. The Bayesian Model Averaging (BMA) multivariable linear regression model is firstly used to evaluate input and output data of the steel structure. Results show that exterior beam members and corner steel columns affect the steel frame the most. This useful result enables the engineer to make reasonable decisions in the selection of input data when simulating design and to select the optimal solution during actual maintenance of structural steel frames.

2. Refined plastic-hinge analysis method

2.1. Formulate system tangent stiffness matrix

The refined plastic hinge approach introduced by Liew et al. [19] is the most effective advanced analysis method for determining the ultimate strength of steel frames. Using stability functions [43], this model adequately captures the geometric nonlinearity caused by the interaction between axial force and bending moments (p-δ effect). The incremental form of the relationship between the member's fundamental force and deformation of a three-dimensional (3-D) beam-column element can be described as shown in [44]. Nonlinear material characteristics include steel's gradual yielding in response to residual stresses and flexure. Consideration is given to the gradual yielding caused by residual stresses using the Column Research Council tangent modulus concept CRC - E_t [45]. The gradual loss of stiffness of a plastic hinge due to flexure is represented by a parabolic function connected with the yield surfaces at the two end portions of a member. In this investigation, the yield surface given by Orbison et al. [46] which has been shown to accurately characterize the inelastic behavior of light to medium weight wide flange sections was employed. Since the inelastic behavior is considered to be lumped at the two ends of the member, this method is advantageous in that it is straightforward in formulation and execution and, more importantly, it requires the fewest number of elements for modeling [47]. The relationship between force and displacement for the beam-column element *i-j* is given as

$$\begin{Bmatrix} P \\ M_y^i \\ M_y^j \\ M_z^i \\ M_z^j \\ T \end{Bmatrix} = \begin{bmatrix} \frac{E_t A}{L} & 0 & 0 & 0 & 0 & 0 \\ 0 & k_{1y} & k_{2y} & 0 & 0 & 0 \\ 0 & k_{2y} & k_{3y} & 0 & 0 & 0 \\ 0 & 0 & 0 & k_{1z} & k_{2z} & 0 \\ 0 & 0 & 0 & k_{2z} & k_{3z} & 0 \\ 0 & 0 & 0 & 0 & 0 & \frac{GJ}{L} \end{bmatrix} \begin{Bmatrix} \delta \\ \theta_y^i \\ \theta_y^j \\ \theta_z^i \\ \theta_z^j \\ \phi \end{Bmatrix}. \tag{1}$$

where

$$k_{1y} = \eta^i \left(S_{1y} - \frac{S_{2y}^2}{S_{1y}} \left(1 - \eta^j\right) \right) \frac{E_t I_y}{L} \tag{2a}$$

$$k_{2y} = \eta^i \eta^j S_{2y} \frac{E_t I_y}{L} \tag{2b}$$

$$k_{3y} = \eta^j \left(S_{1y} - \frac{S_{2y}^2}{S_{1y}} \left(1 - \eta^i\right) \right) \frac{E_t I_y}{L} \tag{2c}$$

$$k_{1z} = \eta^i \left(S_{1z} - \frac{S_{2z}^2}{S_{1z}} \left(1 - \eta^j\right) \right) \frac{E_t I_z}{L} \tag{2d}$$

$$k_{2z} = \eta^i \eta^j S_{2z} \frac{E_t I_z}{L} \tag{2e}$$

$$k_{3z} = \eta^j \left(S_{1z} - \frac{S_{2z}^2}{S_{1z}} \left(1 - \eta^i\right) \right) \frac{E_t I_z}{L} \tag{2f}$$

where P, M_y^i, M_y^j, M_z^i, M_z^j, and T are the axial force, end bending moments at node i and j with respect to weak axis (y) and strong axis (z), and torsion, respectively. δ, θ_y^i, θ_y^j, θ_z^i, θ_z^j and ϕ are the incremental axial displacement, the joint rotations at node i and j with respect to y and z axes, and angle of twist. The sign convention for the positive directions of the basic forces and displacements on the beam-column element as shown in Fig. 1. A is area, $I_y$andI_z are moments of inertia with respect to y and z axes, J is torsional modulus, and L is length of beam-column element, G is shear modulus of material. The shear deformation appears in the modified stiffness matrix by adding the slope of the neutral axis due to shear forces into the total rotations at two ends

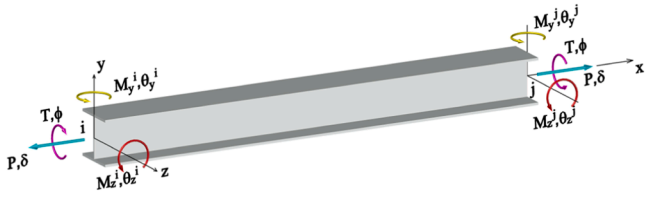

Fig. 1. 3D beam-column element.

of element as following.

The total rotations at the two ends i and j corresponding to $n = (y, z)$ axes given as

$$\begin{Bmatrix} \theta_n^i \\ \theta_n^j \end{Bmatrix} = \begin{Bmatrix} \theta_{Mn}^i \\ \theta_{Mn}^j \end{Bmatrix} + \begin{Bmatrix} \theta_{Sn}^i \\ \theta_{Sn}^j \end{Bmatrix} \tag{3}$$

in which

$$\begin{Bmatrix} \theta_{Mn}^i \\ \theta_{Mn}^j \end{Bmatrix} = \begin{bmatrix} \dfrac{k_{3n}}{k_{1n}k_{3n} - k_{2n}^2} & \dfrac{-k_{2n}}{k_{1n}k_{3n} - k_{2n}^2} \\ \dfrac{-k_{2n}}{k_{1n}k_{3n} - k_{2n}^2} & \dfrac{k_{1n}}{k_{1n}k_{3n} - k_{2n}^2} \end{bmatrix} \begin{Bmatrix} M_n^i \\ M_n^j \end{Bmatrix} \tag{4}$$

$$\begin{Bmatrix} \theta_{Sn}^i \\ \theta_{Sn}^j \end{Bmatrix} = \begin{bmatrix} \dfrac{1}{GA_{Sn}} & \dfrac{1}{GA_{Sn}} \\ \dfrac{1}{GA_{Sn}} & \dfrac{1}{GA_{Sn}} \end{bmatrix} \begin{Bmatrix} S_n^i \\ S_n^j \end{Bmatrix} = \begin{bmatrix} \dfrac{1}{GA_{Sn}L} & \dfrac{1}{GA_{Sn}L} \\ \dfrac{1}{GA_{Sn}L} & \dfrac{1}{GA_{Sn}L} \end{bmatrix} \begin{Bmatrix} M_n^i \\ M_n^j \end{Bmatrix} \tag{5}$$

where θ_{Mn}^i, θ_{Mn}^j, θ_{Sn}^i, and θ_{Sn}^j are the slope of the neutral axis due to the bending moment and the shear forces; GA_{Sn} is shear rigidity concerning n axes, S_n^i, S_n^j, M_n^i, and M_n^j are the shear forces and bending moments at two ends. By substituting Eqs. (4) and (5) into (3), then invert the obtained relation we have the basic force and deformation relationship including shear deformation as

$$\begin{Bmatrix} M_{\mathrm{n}}^i \\ M_{\mathrm{n}}^j \end{Bmatrix} = \begin{bmatrix} \dfrac{k_{1n}k_{3n} - k_{2n}^2 + k_{1n}GA_{Sn}L}{k_{1n} + k_{3n} + 2k_{2n} + GA_{Sn}L} & \dfrac{-k_{1n}k_{3n} + k_{2n}^2 + k_{1n}GA_{Sn}L}{k_{1n} + k_{3n} + 2k_{2n} + GA_{Sn}L} \\ \dfrac{-k_{1n}k_{3n} + k_{2n}^2 + k_{2n}GA_{Sn}L}{k_{1n} + k_{3n} + 2k_{2n} + GA_{Sn}L} & \dfrac{k_{1n}k_{3n} - k_{2n}^2 + k_{2n}GA_{Sn}L}{k_{1n} + k_{3n} + 2k_{2n} + GA_{Sn}L} \end{bmatrix} \begin{Bmatrix} \theta_{\mathrm{n}}^i \\ \theta_{\mathrm{n}}^j \end{Bmatrix} \tag{6}$$

Eq. (6) is extended by constructing the stiffness matrix of general beam-column elements as follows:

$$\begin{Bmatrix} P \\ M_{\mathrm{y}}^i \\ M_{\mathrm{y}}^j \\ M_{\mathrm{z}}^i \\ M_{\mathrm{z}}^j \\ T \end{Bmatrix} = \begin{bmatrix} \dfrac{E_{\mathrm{t}}A}{L} & 0 & 0 & 0 & 0 & 0 \\ 0 & C_{1\mathrm{y}} & C_{2\mathrm{y}} & 0 & 0 & 0 \\ 0 & C_{2\mathrm{y}} & C_{3\mathrm{y}} & 0 & 0 & 0 \\ 0 & 0 & 0 & C_{1\mathrm{z}} & C_{2\mathrm{z}} & 0 \\ 0 & 0 & 0 & C_{2\mathrm{z}} & C_{3\mathrm{z}} & 0 \\ 0 & 0 & 0 & 0 & 0 & \dfrac{GJ}{L} \end{bmatrix} \begin{Bmatrix} \delta \\ \theta_{\mathrm{y}}^i \\ \theta_{\mathrm{y}}^j \\ \theta_{\mathrm{z}}^i \\ \theta_{\mathrm{z}}^j \\ \phi \end{Bmatrix} \tag{7}$$

where C denotes the modified stiffness matrix factors corresponding to Eq. (1) to consider the shearing deformation effect.

According to the CRC concept, E_{t} is tangent modulus used to account for gradual yielding effects caused by residual stresses over the length of members subjected to axial loads between two plastic hinges. When this model contains the right geometrical imperfections, it can provide a very excellent comparison to the plastic zone solutions [48]. According to Liew et al. [23], the CRC - E_t can be expressed as follows:

$$\begin{cases} E_{\mathrm{t}} = 1.0E \text{ if } P \le 0.5P_{\mathrm{y}} \\ E_{\mathrm{t}} = 4\dfrac{P}{P_{\mathrm{y}}}\left(1 - \dfrac{P}{P_{\mathrm{y}}}\right)E \text{ if } P > 0.5P_{\mathrm{y}} \end{cases} \tag{8}$$

where E is elastic modulus of material and P_{y} is squash load.

In Eq. (2.a-f), $S_{1\mathrm{y}}$,$S_{2\mathrm{y}}$,$S_{1\mathrm{z}}$,and$S_{2\mathrm{z}}$ are the stability function capturing for the geometric nonlinear effect [44]; η^{i},andη^{j} are scalar parameters that provide a gradual decrease in the inelastic stiffness of the element due to plastification at ends i and j, respectively. When the force-state parameter α is less than 0.5, indicating that the element is still in an elastic state, these terms are equal to 1.0. They decrease gradually to zero according to the relation $\eta = 4\alpha(1 - \alpha)$ when α is larger than 0.5; that is, the end section of the element begins to plasticize until it becomes a complete plastic hinge. The parameter α is expressed by Orbison's yield surfaces [46] as

$$\alpha = 1.15p^2 + m_z^2 + m_y^4 + 3.67p^2m_z^2 + 3.0p^6m_y^2 + 4.65m_z^4m_y^2 \tag{9}$$

with $p = \frac{P}{P_y}$, $m_y = \frac{M_y}{M_{py}}$ for weak axis, $m_z = \frac{M_z}{M_{pz}}$ for strong axis; in which M_{py} and M_{pz} are plastic moment capacity of cross-section about y and z axes, respectively.

To consider the effect of local and lateral torsional buckling, we use the practical LRFD equations [49] to determine the local buckling strength, M_{nl}, and the lateral torsional buckling strength, M_{nt}. For the local buckling effect, advanced analysis uses the local buckling strength M_{nl} determined by the following equation

$$M_{nl} = \begin{cases} M_p & \text{if } \lambda \le \lambda_p \\ M_p - \left(M_p - M_r\right)\left(\dfrac{\lambda - \lambda_p}{\lambda_r - \lambda_p}\right) & \text{if } \lambda_p < \lambda \le \lambda_r \\ S_xF_{cr} & \text{if } \lambda > \lambda_r \end{cases} \tag{10}$$

where M_p and M_r are plastic moment and limiting buckling moment, respectively; λ, λ_p, and λ_r are slenderness, limiting slenderness for a compact section, and limiting slenderness for a noncompact section, respectively. S_x is elastic section modulus about major axis; and F_{cr} is the critical stress.

For the lateral-torsional buckling effect, the nominal buckling strength M_{nt} is determined using the following equation

$$M_{nt} = \begin{cases} M_p & \text{if } L_b < L_p \\ C_b\left[M_p - \left(M_p - M_r\right)\left(\dfrac{L_b - L_p}{L_r - L_p}\right)\right] & \text{if } L_p \le L_b \le L_r \\ C_b\dfrac{\pi}{L_b}\sqrt{EI_yGJ + \left(\dfrac{\pi E}{L_b}\right)^2 I_yC_w} & \text{if } L_b > L_r \end{cases} \tag{11}$$

where L_b, L_p, and L_r are distance between points braced to prevent twist of the cross section, limiting laterally unbraced length for I-shaped members, and limiting laterally unbraced length for doubly symmetric I-shaped members, respectively; C_b is a lateral-torsional buckling modification factor non-uniform moment diagrams; E, I_y, G, J, and C_w are elastic modulus, moment of inertia about y-axis, shear modulus of elasticity of steel, torsional constant, and warping constant, respectively.

When the local buckling and the lateral-torsional buckling are considered, the plastic moment, M_{pz}, of Eq. (9) is replaced by the buckling strength $M_n = \min(M_{nl}, M_{nt})$ [50,51].

Eq. (1) provides the tangent stiffness matrix after updating to account for the transverse shear deformation effect established in the member's local coordination. The transformation matrix T [44] will transfer it to global coordination via equilibrium and kinematic relations. The structure is regarded to impose no side-sway in the beam-column member during the established procedure. However, because member movement in global coordination causes structural sway, additional axial and shear forces must be supplied to the member. This circumstance is known as the P-Δ effect, and it was accounted for throughout the structure's analysis by including the geometric stiffness matrix $[K_g]_{12\times12}$ [52]. The following is the final tangent stiffness matrix of the beam-column element in global coordinate considering both geometric nonlinear (P-δ, P-Δ) and material nonlinear inelastic effects:

$$[K]_{12x12} = [T]_{6x12}^T[K_e]_{6x6}[T]_{6x12} + [K_g]_{12x12} \tag{12}$$

and the general force-displacement relationship of beam-column element can be written as

$$\{f\} = [K]_{12x12}\{d\} \tag{13}$$

in which $[T]_{6x12}^{T}$ is the transformation matrix, while superscript T indicates the transfer notion. $[K_e]_{6x6}$ is the tangent stiffness matrix of the beam-column element in the local coordinate. $[K_g]_{12x12}$ is a geometric stiffness matrix used to account for large displacement effect in the global coordinate. $\{f\}$and$\{d\}$ are the force and displacement vectors at the element nodes in the global coordinate.

Finally, we derive the system stiffness matrix $[K]$ encompassing the advanced effects of interest by assembling the element tangent stiffness matrices of Eq. (12) and node force vectors in Eq. (13) and then solving the nonlinear problem to find the displacements of the steel frame structure.

2.2. Implementation

For the second order refined plastic-hinge analysis method mentioned above, the relation between a force vector and displacement is nonlinear and the displacement often depend on the displacements at earlier stages. For this reason, we make the problem discrete in time with increments and to achieve equilibrium at the end of the increments, we use an iterative solution algorithm. This method is straightforward in implementation, and efficient in computation. In the incremental procedure, the magnitude of incremental loads specified in the input data is automatically adjusted in the program such that plastic hinges will not form within the load increment predetermined through input data. Thus, subsequent element stiffness formulation will account for stiffness reduction due to the presence of plastic hinges. The analysis program scales a predetermined load increment when the change in the element stiffness parameter exceeds a tolerance which is predefined in the analysis program. This automatic scaling of incremental loads leads to minimize the error in using the simple incremental solution method.

In this study, we apply the two incremental-iterative methods in parallel to make a dual algorithm technique to find the solution vectors. The modified Newton-Raphson algorithm [53] is called for solving nonlinear inelastic problem to determine the maximum response state of the structure under load actions, and then the Generalized Displacement Control method [54] is called to determine the ultimate resistance state of structure. The Stochastic Practical Advanced Analysis Program (SPAAP) is, therefore, developed in random field of input factors in whole structure to find accurate results, reliability index and sensitivity of parameters in straightforward way but high efficiency as follows.

3. Sampling techniques

Several techniques may be utilized to solve the safety structure challenges since the input parameters are uncertain factors that affect the system's true responsiveness, reliability, and sensitivity. The simulation techniques are presented as one feasible way to solve such problems. The essential objective is to numerically simulate a phenomenon and then count the number of times a particular event occurs.

3.1. Monte carlo sampling

The Monte Carlo method is a methodology that allows us to obtain numerical findings without conducting any physical testing. We can use existing experimental results (or other information) to calculate the probability distributions of the main parameters in our situation. After that, the distribution information is used to generate numerical data samples. This strategy is used to address complex issues where closed-form solutions are either impossible or extremely difficult to find. In some cases, if the closed-form solution can be solved (or at least), many simplifying assumptions are made, whereas MCS allow us to investigate the original problem without any assumptions and acquire more realistic conclusions. The sample data sets are generated as follows based on the known probability distribution of uncertain input parameters:

- Generation of Normal Random Numbers:

Because normal probability distribution is most commonly employed in this study, the ability to model normally distributed random variables is crucial. To begin, we must construct a set of standard normal random numbers $z_1, z_2, \ldots, z_n$. To achieve this, we must first generate a series of uniformly distributed random variables $u_1, u_2, \ldots, u_n$ between 0 and 1. Then, for each u_i, we may compute a value z_i as,

$$z_i = \Phi^{-1}(u_i) \tag{14}$$

where Φ^{-1} is the inverse of the standard normal cumulative distributed function. Assuming we have a normally distributed random variable X with mean μ_X and standard deviation σ_X, we can determine the appropriate x_i value using

$$x_i = \mu_X + z_i\sigma_X \tag{15}$$

- Generation of Lognormal Random Numbers

Assume X is a lognormal random variable with a mean μ_X and a standard deviation σ_X. To obtain a sample value x_i, we first construct a sample value u_i of a uniformly distributed random number with a probability such that $0 \le u_i \le 1$. Then, using Eq. (14), a sample value z_i from a standard normal distribution is calculated. Finally, we can deduce x_i from the relationship between normal and lognormal variables as follows:

$$x_i = \exp(\mu_{\ln X} + z_i\sigma_{\ln X}) \tag{16}$$

where

$$\sigma_{\ln X} = \sqrt{\ln\left(V_X^2 + 1\right)} \tag{17}$$

$$\mu_{\ln X} = \ln(\mu_X) - \frac{1}{2}\sigma_{\ln X}^2 \tag{18}$$

in which V_X is the coefficient of variation of random variable X.

3.2. Latin hypercube sampling

The MCS often induces lower convergence rate because of its poor space-filling properties (irregular distribution data), i.e., there are too many sample points in one place while other regions have no sample points. This approach, therefore, has not received an overwhelming acceptance due to the excessive computational effort that is required. Several sampling techniques, called variance reduction techniques, have been developed in order to improve the computational efficiency of MCS by reducing its statistical error and keeping the smallest sample size. Because of its simplicity and efficacy, importance sampling has been the most extensively used variance reduction strategy [55], although it is dependent on the importance function used, which is connected to the simulation's convergence speed and accuracy. When the output contains a large number of random variables with varying probability distributions, selecting the importance function incorrectly may result in incorrect results.

LHS is a stratified sampling technique. In conventional random sampling, new sample points are created without regard for prior sample points, or the number of sample points required. In LHS, one must pick how many sample points to utilize and memorize each one's overall position. Unlike pseudo-random generators, this sampling method assures that the generated samples are more evenly dispersed in the sample space. LHS has two effortless steps: 1) Divide each random variable's range into N equal-mass bins; 2) Generate one sample from each bin. This method has the advantage of reducing statistical variance and converges faster than MCS, yet the random variables are sampled from the entire range of values, guaranteeing that no subdomain is oversampled.

According to the previously mentioned techniques, a subroutine is constructed by the own MATLAB script to produce pseudo - random input parameters into the analysis program for collecting desired

information of interest.

4. Numerical examples and discussions

4.1. Typical space steel frame structure

The purpose of this section is to present the application of the developed program to investigate the stochastic response of steel frame structure compared to the deterministic analysis, and to evaluate the sensitivity and correlation of the input and output parameters. In fact, several different structures have been investigated, for example a two-story frame structure, however, the comparison results showed the same trend. Therefore, in this paper, we only present the analysis results of a six-story steel frame as a typical problem. The 63-member steel structure as shown in Fig. 2 is constructed using A36 steel and W-shaped steel in accordance with AISC Manual [56]. Twelve columns employ W12×87, six columns employ W12×120, twelve columns employ W10×60, nine beams employ W12×53, six beams employ W12×87, and eighteen beams employ W12×26. The types of W-shape steel for each member in this frame were selected by Liew et al. [19]. The material properties of all sections with their nominal values are the yield stress of 250 MPa, the Elastic modulus of 200 GPa, and Poisson's ratio of 0.3. All joints between beam and column are assumed rigid connections and the frame is rigidly fixed to the ground. The nominal gravity load is a uniform floor load of 9.6 kN/m^2 equivalent to concentrated loads applied at the columns of every story. The nominal wind load is assumed as point loads of 53.376 kN applied in Y-direction on the front elevation at all beam-column joints. All columns and beams are considered to be compact and to have sufficient lateral support allowing them to rise to their full plastic moment capabilities without experiencing local and lateral buckling.

4.2. Verification of deterministic analysis

The steel frame used in this study is a popular example as the benchmark frame for progress applications of analysis approach proposed by Orbison [57] who used the basic plastic-hinge approach. Then Liew et al. [19] proposed the direct analysis under the improved plastic hinge technique for this frame. A spread-of-plasticity analysis for the inelastic approach is also introduced by Jiang et al. [15]. Kim et al. [22] used the nonlinear stable functions to evaluate the ultimate response of steel frames. In this study, we use the module of the refined plastic-hinge analysis with one element per member to solve this frame due to the fact that it is easier controllable and accurate enough with concentrated plasticity at the ends of the members [15]. More complicated phenomena like initial imperfections, buckling, and semi-rigid connections were not considered because their effects obviously weaken the system [51, 58].

The deterministic analysis of the steel frame is conducted using the PAAP and its results are then compared to that conducted by the commercial software ABAQUS v6.14 and other research. The comparison is presented in Fig. 3 and Table 1. The relationship of load – displacement curve at node A obtained from the PAAP program is slight deviation compared to Liew et al. (used plastic hinge analysis, −2.02% deviation), Jiang et al. (used plastic zone analysis, −1.39% deviation) and commercial program ABAQUS V6.14 (used beam element B31 with ten elements per member, 0.09% deviation), these results prove reliability of the PAAP in deterministic analysis. However, the time consumed to run one simulation by ABAQUS is longer than the proposed program about 10.8 times. The comparison indicates that the deterministic analysis using PAAP provide a reliable result, thus it can be confidently used for the next simulation.

4.3. Stochastic analysis

In practical design, we normally use the input parameters of material, geometry, and loads as constant factors and the same values are assigned the structural members which have the same kind. But distinctive features always exist in each member due to inevitable uncertainty resources. The combination together in a whole structure is clearly unknown, therefore, the deterministic results may hide the risks for the system. For these situations, we consider the response of the entire structure as random variable in which each input parameter of each individual section is a random variable, and it combines together randomly to form a random structure. The uncertain input parameters vary in their random field with a defined distribution law found by experimental measures in practice. The mean value of the structural response after running a large number of simulations may be considered accurately resistant capacity based on the large number law [59].

In this study, the principal material parameters of structural steel are elastic modulus (E), yield stress (F_y), Poisson's ratio (υ), and shearing modulus (G), whose values are uncertain. Bartlett et al. [27] examined 207 steel coupons and determined that the measurement of E and F_y for each sample has distinct values. By statistical analysis, the mean value,

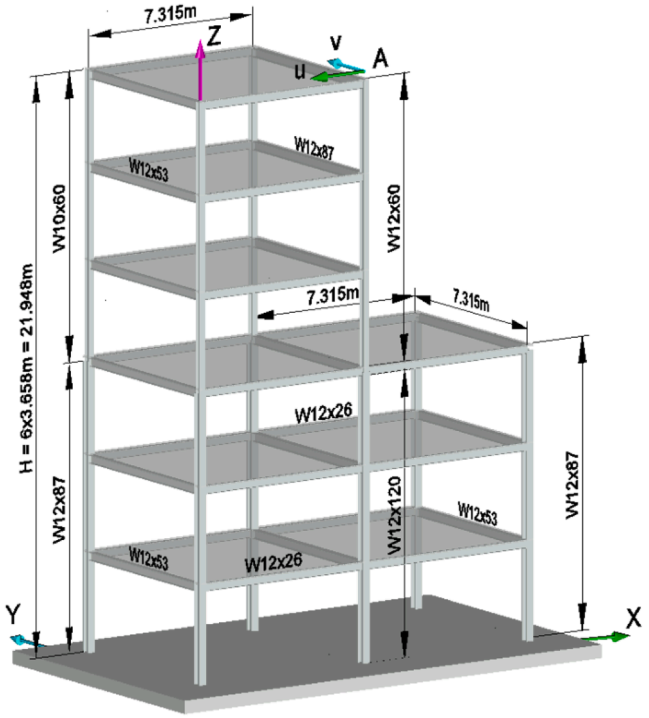

Fig. 2. Six-story space steel frame.

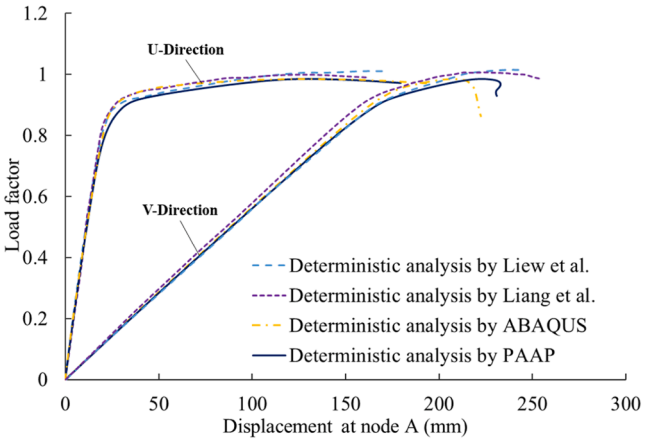

Fig. 3. Load-displacement curves at node A of steel frame.

Table 1
Comparison of deterministic analysis results to PAAP.

Deterministic analysis	Max. load factor	Deviation (%)	Time (s)
Liew et al.	1.005	−2.02	–
Jiang Et al.	0.9986	−1.39	–
ABAQUS – 10 elements	0.9838	0.09	25
PAAP – 1 element	0.9847	–	2.3

bias factor (ratio of mean to nominal value), coefficient of variation (Cov), and lognormal distribution law have been determined (see Table 2). Therefore, each member can be considered as a random variable of E and F_y, creating a total of sixty-three random members per simulation of the steel frame. Due to its slight change, the Poisson's ratio assumes as a constant value, but the shearing modulus depends on the variability of E through the deterministic expression $G = \frac{E}{2(1+\vartheta)}$.

The geometrical section characteristics include cross-section area (A), bending inertia about y and z axes (I_y, I_z), shear area along y and z axes (S_{ay}, S_{az}), plastic section modulus about y and z axes (Z_{py}, Z_{pz}), section modulus about y and z axes (S_y, S_z), and torsional modulus (J). These characteristics are expressed via deterministic expressions that depend on cross-sectional dimensions. In reality, the cross-sectional dimensions are uncertain measured values making geometrical section characteristics to be uncertain. Melcher et al. [26] evaluated the variability of shaped steel dimensions and their correlation based on 371 measurements and statistical characteristics. Because there are the strong correlations between width of the upper and the lower flanges as well as the thickness of the upper and lower flanges, we only consider the independent randomness of four primary dimensions of height (H), width (B), flange thickness (t_f), and web thickness (t_w) whose values vary according to the Gaussian distribution (see Table 3). Since the dimensions of the section fit the Normal distribution law, the geometrical section characteristics obey the Normal distribution as well, according to the central limit theorem [60].

In the static analysis of steel frame structures, we frequently consider two common loads of the dead load, and the live load, in despite of the fact that structures are subject to the variety of loads. Typically, the dead load in design is the self-weight of the structural and nonstructural parts that are permanently attached to the structure. Due to the varying degrees of variance among structural and nonstructural elements, it is extremely challenging to precisely determine their magnitudes. Therefore, all components of the dead load are regarded as normal random variables [28] (see Table 4) with varying random magnitudes at every location on the structure. The wind load on a structure depends on a number of characteristics, including wind speed, wind direction, local topography, and a number of other variables. For design reasons, the wind pressure on the exterior surfaces of a structure is first estimated, and then converted to loads. Due to the fact that wind load varies according to the extreme value type I distribution [28] in a given time interval, we may estimate the instantaneous extreme magnitude of wind load and assume it to be constant for the analysis.

On practical constructions, we cannot anticipate what instantaneous combination would occur at the moment of analysis; thus, we typically utilize their nominal values instead. Due to the inability to conduct actual experiments, it is better to investigate the random strength of the steel frame using the probability models in this instance. These input parameters are consequently modeled as random variables using the crude MCS approach coupled with the variance reduction method of LHS. The load-displacement curve for each numerical simulation has been computed by the PAAP program, and the precise result of steel frame strength is a statistical convergence after n_{sim} pseudo-random samples under the law of large numbers [59] as follows:

$$\lim_{n \to n_{\text{sim}}} \Pr(|\overline{R}_n - \mu| < \varepsilon) = 1 \tag{19}$$

where $\overline{R}_n$ is the average response of the system's ultimate strength, μ is expected value, n is the number of simulation, and ε is specified nonzero margin. As illustrated in Fig. 4, the convergence rate of the crude MCS and the technique of LHS simulations is compared. If we choose a very small nonzero margin of $\varepsilon = 10^{-7}$, the LHS simulation requires 321 pseudo-random samples to converge to the expected value, whereas the crude MCS simulation requires 418 samples to achieve the same result. It demonstrates that the LHS is approximately 30% more efficient than the crude MCS in terms of the number of simulations; hence, the LHS is chosen for the other simulations in this study.

As shown in Table 5, the SPAAP is executed multiple times to evaluate the confidence of the probability model and to compare the outcomes of the crude MCS simulation to the LHS simulation. The convergence of the maximum load factor after a number of runs, with a deviation of less than 0.01 percent, demonstrated that the probability model is accurate enough to determine the precise steel frame strength. The comparison between the stochastic results and that of deterministic as shown in Fig. 5 reveals that the ultimate load-carrying capacity using the stochastic analysis tends to underestimate the nominal result approximately 3.62%. Thus, the effect of uncertain input parameters is considerable in practical design.

4.3. System reliability analysis

The uncertainty of input parameters makes the response of system to be unpredictable both its demand and resistance. Consequently, total safety cannot be attained, which necessitates that structures be constructed with an "acceptable low" probability of failure [61]. In the context of structural reliability assessments, a limit state function represents the border between the desired and undesirable performance of the structures in order to characterize failure. Let the probability of failure (P_f) be a function involving many random variables, and let P_f be defined as follows:

$$P_f = P(R - S \le 0) = P(Q(R,S) \le 0) = \int F_R(x) f_S(x) dx \tag{20}$$

where R and S represent the system resistance and total load effect, respectively, whose values rely on the unpredictability of the uncorrelated variables E, F_y, H, B, t_f, t_w, D, and W [26]. $Q(R,S)$ is the limit state (performance) function whose value corresponds to the difference between R and S. $F_R(x)$ represents the cumulative distribution function of R, while $f_S(x)$ represents the probability density function of S. Several methods exist for calculating the probability of failure for various prevalent types of limit state functions found in practice. The application of the simultaneous equation approach or the matrix approach to determine P_f is either extraordinarily difficult or impossible for structural engineering problems with so many random variables. In such cases, MCS is the only feasible method for determining P_f or the reliability index β [62]. The probability of failure can be expressed by

Table 2
Statistical properties of material variables.

Property	Variable	Nominal	Bias factor	Cov.	Distribution	Reference
Elastic modulus	E	200 (GPa)	0.993	0.034	Lognormal	[27]
Yield stress	F_y	250 (MPa)	1.002	0.06	Lognormal	[27]
Poisson's ratio	υ	0.3	1.0	0	Constant	Assumed
Shearing modulus	G	76.923 (GPa)	1.0	0.034	Lognormal	Dependence

Table 3
Statistical properties of cross-sectional dimension variables.

Dimension	Variable	Nominal W12×87	W12×120	W10×60	W12×53	W12×26	Bias factor	Cov.	Distribution	Ref.
Height	H (mm)	318.00	333.26	259.49	307.82	310.37	1.001	0.0044	Normal	[26,56]
Width	B (mm)	307.82	312.91	256.94	254.40	160.02	1.012	0.0103	Normal	[26,56]
Flange thickness	t_f (mm)	20.61	28.24	17.30	14.63	9.67	0.998	0.0480	Normal	[26,56]
Web thickness	t_w (mm)	13.10	18.06	10.68	8.78	5.85	1.055	0.0418	Normal	[26,56]

Table 4
Statistical properties of loads.

Load	Variable	Nominal	Bias factor	Cov.	Distribution	Reference
Dead load	D	9.6 (kN/m^2)	1.05	0.1	Normal	[28]
Wind load	W	53.376 (kN)	0.85	0.35	Gumbel	[28]

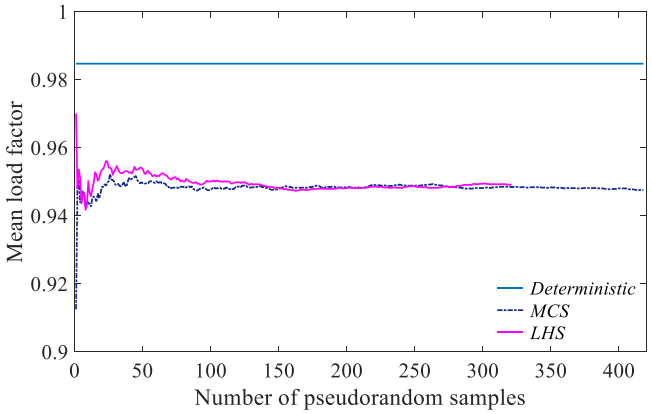

Fig. 4. Convergence rate of numerical simulation methods.

Table 5
Convergence of LHS and crude MCS simulations.

Stochastic analysis		Max. load factor	Deviation (%)	Time (s)
SPAAP_LHS	1000 samples	0.9493	0.01	5621.9
	5000 samples	0.9491	−0.01	28,034.2
	10,000 samples	0.9493	0.01	54,652.2
SPAAP_MCS	1000 samples	0.9499	0.02	5619.9
	5000 samples	0.9496	−0.01	28,175.4
	10,000 samples	0.9497	0	56,350.8

$$P_f = \frac{N_f}{N} \tag{21}$$

where N_f is number of simulations when the structure failed and N is the total number of simulations. The reliability index β is related to the probability of failure by

$$\beta = -\Phi^{-1}(P_f) \tag{22}$$

where $\Phi^{-1}(.)$ is the inverse of the standard normal cumulative distribution function [61].

Initially, the MCS using the variance reduction method of the LHS technique, which is developed in MATLAB, is used to generate the random variables. Then, the SPAAP is invoked to execute the probabilistic model with these simulated input parameters by the dual analysis algorithms. The mNR algorithm helps to define the set of the maximum demand displacement of the frame under acting loads and the GDC algorithm helps to determine the set of ultimately resistant displacement

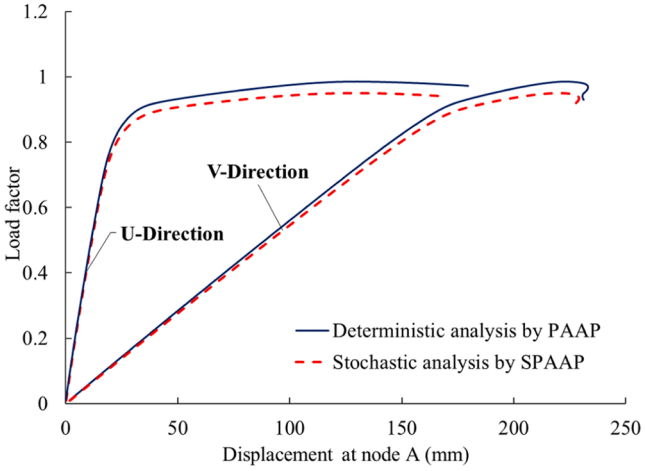

Fig. 5. Deterministic and stochastic load-displacement curves at node A on X and Y axes.

of structure at the time of collapse due to plastic mechanism. The set of limit states of the structure is determined by the difference between the displacement values of resistance and the demand. Lastly, the resistance, demand, and performance data are plotted as shown in Fig. 6. The probability of failure, $P(Q(R,S) < 0)$, can be determined by reading the probability value at the point where a vertical line passes through the origin crosses the plotted data curve. Eq. (22) indicates that a reliability index corresponds to the value of the normal standard variable at the point of intersection.

As shown in Table 6, it can be seen that the steel frame structure's reliability index remains outside the range of the required target reliability index for the strength of the limit state. In accordance with the LRFD specification, the target reliability indices for steel members range between 2.5 and 3.0 [28], equating to a failure probability between 0.62 and 0.13 percent. Due to the advantageous effects of force redistribution, the system reliability of redundant structures is generally greater than that of a single member. The displacement-based reliability index for steel frame is an efficient and accurate solution for system reliability analysis based on numerical simulation and probability model in conjunction with advanced analysis methods.

4.4. Sensitivity and correlation of uncertain input parameters

4.4.1. Sensitivity in terms of coefficients of variation

Sensitivity measurements connected to failure probability, or a certain limit state function are not the only things that designers are interested in. There are numerous instances where the impact of various basic variables on diverse types of structural responses is investigated. In general, it is a problem involving a function of random variables that represents a variable R response. The following are some sensitivity measures that can be used to estimate the impact of randomness on the response variable. MCS approaches provide a straightforward way to handle such challenges, and the LHS currently appears to be the most successful technique for estimating statistical parameters of structural response [63].

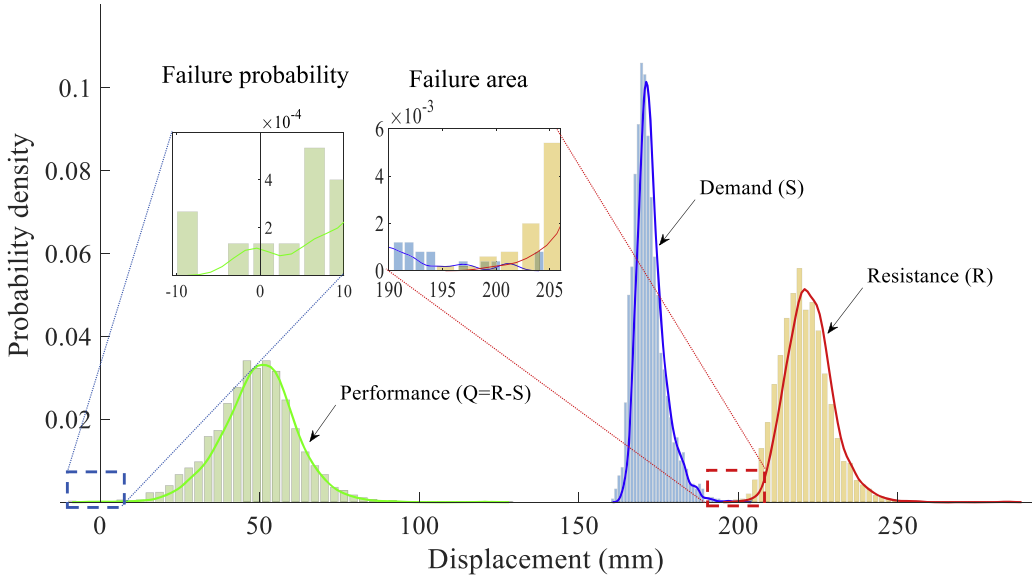

Fig. 6. Probability of failure for six-story steel frame structure.

Table 6
Probability of failure and system reliability index.

Number of simulation	Number of failure	Failure probability	Reliability index	Target reliability
2500	3	0.12%	3.04	2.5 – 3.0
5000	3	0.06%	3.24	
10,000	5	0.05%	3.29	

The statistical evaluation of the set of simulated response variables R_j $(j = 1, 2, \ldots, n)$, where n is the number of simulations, and their means and coefficients of variation are presented in Table 7. We designate the partial coefficient variation v_{R_i} for the scenarios where the simulation process treats only the variable $X_i = (E, F_y, H, B, t_f, t_w, L)$ as random. Other basic variables are maintained at their nominal values. These factors demonstrate the relative impact of random input variables on the unpredictability of structural response. According to Novak et al. [64], the approximate formula for the coefficient of variation of the response variable in the case of compound variable v_R is as follows:

$$v_R^2 \cong \sum_{i=1}^{7} v_{R_i}^2 \tag{23}$$

As shown in Fig. 7, such sensitivity can be easily depicted using pie charts, as shown in Eq. (23). The results show that, among the individual basic variables, yield stress has the highest sensitivity with a ratio of approximately 60.6%, followed by flange thickness of shaped steel with a ratio of approximately 26.6%, followed by loads with a sensitivity ratio of approximately 7.6%, and the remaining variables have small sensitivities, indicating a negligible influence on the resistance of steel structures, as showed in Fig. 7a. Among the group variables, the composition of material properties has the greatest influence (63.2%), followed by geometrical characteristics (29.2%), and finally loads (7.6%), as showed in Fig. 7b.

Table 7
Coefficients of variation of response variables and Shapiro-Wilk normality test.

Scenario	Variable	Mean	COV	P value	Distribution
Elastic modulus	v_{RE}	0.9633	0.0037	0.069	Normal
Yield stress	v_{RF_y}	0.9641	0.0178	0.052	Normal
Height	v_{RH}	0.9643	0.0016	0.918	Normal
Width	v_{RB}	0.9643	0.0028	0.504	Normal
Flange thickness	v_{Rt_f}	0.9637	0.0118	0.273	Normal
Web thickness	v_{Rt_w}	0.9643	0.0017	0.512	Normal
Loads	v_{RL}	0.9543	0.0063	0.279	Normal
Compound	v_R	0.9514	0.0228	0.071	Normal

Sensitivity data is expected to have a significant impact on the development of technological processes and on manufacturing of building materials and structures. It is possible to plan and organize the checking and inspection activities in a way that leads to more consistent constructions because of the varied sensitivity of the structural response.

4.4.2. Correlation analysis

Measures of sensitivity can offer designers with valuable information by focusing resources on decreasing uncertainty in the most sensitive parameters, not just for individual failure modes but also for the probabilities of system failure. However, this only indicates the degree of influence of the input variables on the structural system's behavior and not the degree of mutual correlation between the basic input variables and the system's overall behavior. A linear correlation research based on statistical theory is necessary to provide light on this question. To investigate this linear correlation, a statistical set of critical responses of steel structure frames affected by uncertainty in input parameters of single variables X_i and compound variables X are employed. In accordance with the law of large numbers, the distribution of sample data tends to approach the normal distribution as the number of samples increases to infinity [59], however a test procedure is required to ensure that the outcome data adhere to Gaussian distribution laws. We therefore employ the R-programming with application of Shapiro-Wilk normality test to confirm this issue [65]. According to test data presented in Table 7, the P-value of all scenarios is greater than 0.05, indicating that the outcome data has passed the significance test or that the distributions comply with the normal distribution. These median values are not statistically different, and the distribution data is concentrated also indicating that these distributions correspond to the normal distribution (see Fig. 8). As a result, the Pearson correlation coefficient (r) can be used to evaluate the relationship between any couple of variables. Using the following formula, the Pearson correlation coefficient was calculated:

$$r = \frac{\sum_{i=1}^{n}(x_i - \bar{x})(y_i - \bar{y})}{\sqrt{\sum_{i=1}^{n}(x_i - \bar{x})^2 \sum_{i=1}^{n}(y_i - \bar{y})^2}} \tag{24}$$

where n is sample size; x_i and y_i are the individual sample points indexed with i of random response variable x and y; and $\bar{x}$ and $\bar{y}$ are the sample

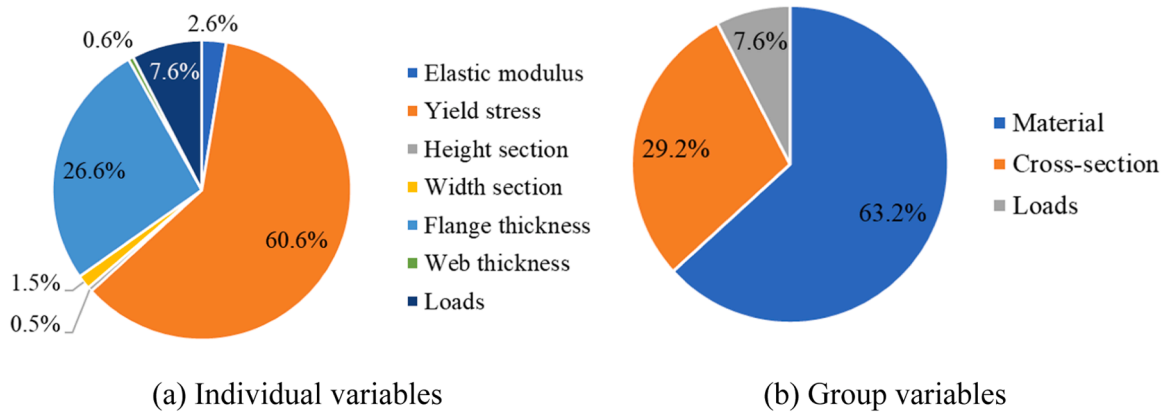

Fig. 7. Sensitivity levels of scenarios in randomness.

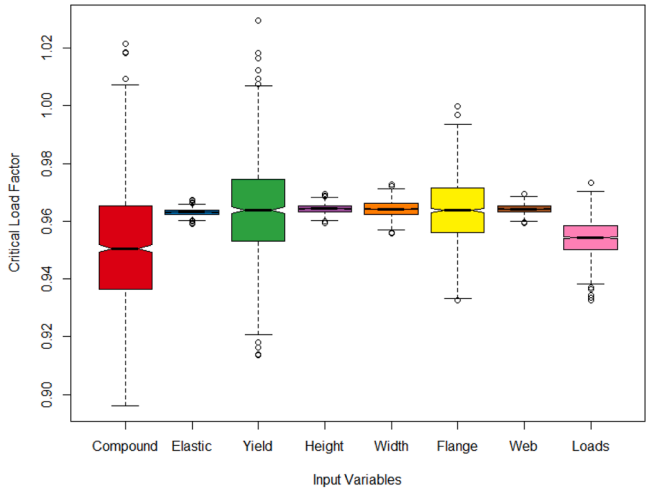

Fig. 8. Distribution of response variables.

means of response variables x and y.

The value of the correlation between response variables is calculated using R-programming as presented in Fig. 9. The results demonstrate that there is not mutual correlation between the effect of individual input parameters on the ultimate resistance of the structure. The yield stress of the material shows a high correlation with the structure's resistance, $r_{fy} = 0.78$ close to 1.0, which is consistent with the sensitivity analysis results in terms of coefficient of variation. In other words, the higher the yield stress of the steel, the stronger the resistance of the structural frame. This is a clear indicator to help the engineer better selecting a solution to increase the load carrying capacity of the steel structure frames. The uncertainty of cross-sectional dimensions does not have any significant sensitivity to the behavior of the system. Their linear correlation coefficient is small, close to zero, showing that the uncertainty in the size of the members does not considerably effect on the ultimate load-carrying capacity of the steel frame. The correlation coefficient between external load and resistance of the steel frame is very low as $r_L = 0.23$. It can be concluded that the resistance of a steel frame is not a function of external loading.

The investigation of the correlation coefficient between the effects of input variables on the resistance of the structural steel frame indicates that selecting a steel material with a high yield strength is more effective than enlarging the cross-sectional dimensions of the members. In order to precisely manage the ultimate resistance of steel frames, it is preferable to control the material properties, particularly yield strength, as opposed to the geometrical characteristics of the members. In addition, it is recommended that the self-weight be carefully evaluated, since it tends to result in an overestimation of the actual load capacity of the steel structures.

4.4.3. *Predictive models of bayesian model averaging method*

The results of the sensitivity analysis in terms of the coefficient of variation can provide the ranking of the uncertain input parameters according to their sensitivity. The Pearson correlation coefficient is employed to evaluate the relation between input variables and the limit state analysis of steel structural frames. In order to better control the analysis and design outcomes for complex steel frames consisting of many components, it is crucial to identify sensitive and highly correlated individual portions or components in a steel frame. Focusing on the precise processing of these input parameters at structural components that have a substantial impact on the overall structural behavior would reduce design risks and shorten the maintenance time of steel structure frames in practice. For these reasons, we employ the multi-variable linear regression Bayesian Model Average (BMA) [66] to predict the potential models which forecast the most information on the structural response based on individual features of components through their weighted factors.

Based on the set of input data, $X = (E, F_y, H, B, t_f, t_w, L)$ is generated by MCS simulation to find the set of critical load factor λ by the SPAAP. If we let $M = \{M_1, M_2, \ldots, M_K\}$ to denote the set of all potential models, the posterior distribution of λ given the data X is

$$p(\lambda|X) = \sum_{k=1}^{K} p(\lambda|M_k, X)p(M_k|X) \tag{25}$$

in this equation, each model's predictions, $p(\lambda|M_k,X)$, are weighted by the model's posterior model probability, $p(M_k|X)$. This term is derived by re-applying the Bayes rule, but this time at the level of models rather than parameters

$$p(M_k|X) = \frac{p(X|M_k)p(M_k)}{\sum_{l=1}^{K} p(X|M_l)p(M_l)} \tag{26}$$

where

$$p(X|M_k) = \int p(X|\beta_k, M_k)p(\beta_k|M_k)d\beta_k \tag{27}$$

Eq. (25) is the marginal likelihood of model M_k, β_k is the vector of parameters of model M_k, $p(\beta_k|M_k)$ is the prior density of β_k under model M_k, $p(X|\beta_k,M_k)$ is the likelihood, and the $p(M_k)$ is the prior probability that M_k is the true model. M, the set of all models under consideration, is implicitly conditional on all probabilities. M is defined as the set of all feasible combinations of predictors in this investigation.

With these preliminary considerations, one comes at an obvious approach of contrasting two distinct models, which is as follows: Calculating the ratio of the posterior model probability of the alternative

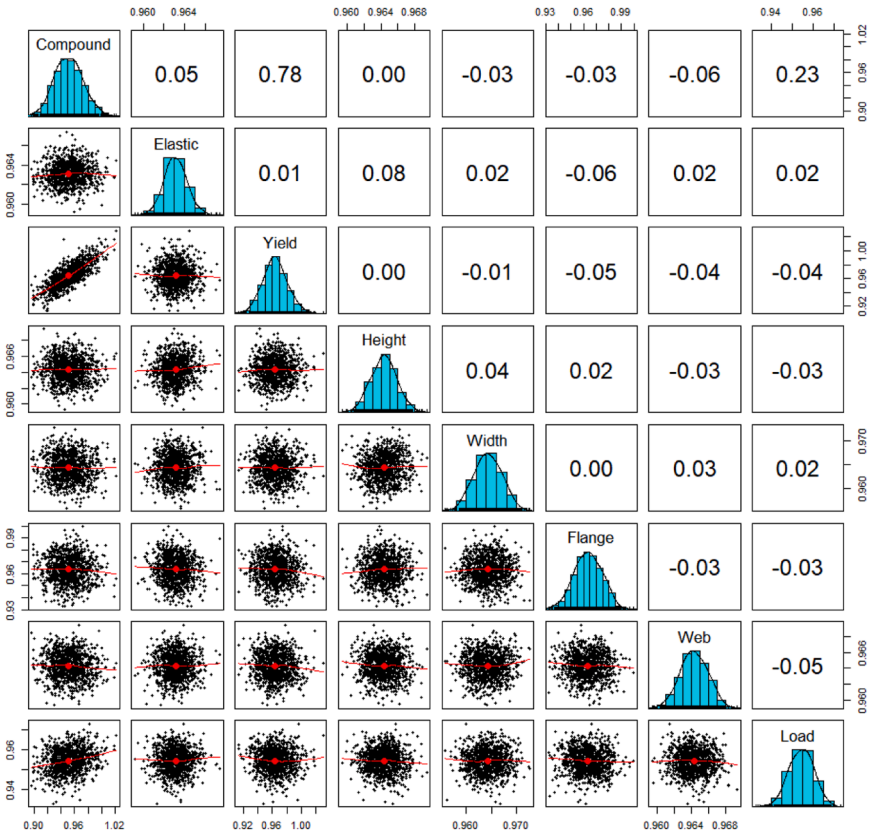

Fig. 9. Pearson correlation coefficient of any two variables.

model, M_k, to the posterior model probability of the null model, M_l, is all that has to be done. This results in

$$\frac{p(M_k|X)}{p(M_l|X)} = \frac{p(X|M_k)}{p(X|M_l)} \times \frac{p(M_k)}{p(M_l)} = BF_{10} \times \frac{p(M_k)}{p(M_l)} \tag{28}$$

where BF_{10} is the Bayes factor, the ratio on the right hand side is the prior model odds, and the ratio on the left hand side is posterior model odds. Each of the models that we are taking into consideration is of the form

$$\boldsymbol{\lambda} = \beta_0 + \sum_{i=1}^{m} \beta_i \boldsymbol{X}_i + \varepsilon = \boldsymbol{X}\boldsymbol{\beta} + \varepsilon \tag{29}$$

where $\boldsymbol{X}$ is a $n\ x\ (m\ +\ 1)$ matrix containing the observed data on m predictors. The n vector λ contains the observed data on the dependent variable. We give ε a normal distribution with a mean of zero and a variance of σ^2, and we suppose that the $\varepsilon's$ in different circumstances are independent. The $(m + 1)$ individual parameters β and σ^2 are assumed to be unknown.

The Bayes Information Criterion (BIC) is utilized by the Bayesian Model Averaging (BMA) algorithm to organize the models from lowest to highest corresponding to their model parameters. The frequency of occurrence of each input parameter and its location within the ideal models, as well as their weighted factors, will reveal the level of influence on the structure's ultimate resistance.

This paper employs a typical steel frame construction to investigate a numerical model with 63 members corresponding to 408 random variables for each simulation (i.e., there are 408 sets of input data of X). To facilitate the process of selecting optimal models, we divide the structure into six main groups based on the shaped steels used for Beams and Columns (W12×87C, W12×87B, W12×53B, W12×120C, W12×26B, and W10×60C), with each group containing six input parameters (E, F_y, H, B, t_f, t_w), and a set of load variables (L). Thus, we are left with thirty-seven sets of predictors in order to locate the optimal models using the BMA technique. The R programming language is utilized to identify probable models that might be used to understand the ultimate resistance of a structure with minimal input parameter variables.

The BMA method identifies 340 potential models, of which five are selected as the best based on evaluation according to BIC criteria, determination factor (R^2), and the number of variables needed to predict results (see Table 8). Notably, the variables are related to the material's intensity and the flange thickness of the shaped steels, which occur with a probability of one hundred percent in any possible model. This conclusion corresponds with the findings of the sensitivity analysis and the Pearson correlation coefficient. In addition, the BMA method gives proof of the structural components that are most susceptible to the structural steel frame's strength. Model 1 is considered the best model based on the smallest BIC index, and it only requires five input variables to explain approximately 21.9% of the steel frame; nevertheless, its posterior probability is just about 1.9%. Other models' capacity to explain the steel frame's resistance is approximately 0.5% to 1% stronger than Model 1, despite the fact that these models require more predictors (6–7 variables) than Model 1 (5 variables). Importantly, we have the results of the BMA analysis, which is utilized to identify the components or members that have the largest impact on the steel frame's ultimate strength.

According to the detailed results in Table 8, the yield stress of the W12×53 shaped steel beams and the W12×87 corner columns is remarkable. In the predicted models, their expected linear regression coefficients are 1.52e-3 with a standard deviation of 1.2e-4 and 1.11e-3 with a standard deviation of 1.35e-4, respectively. The flange thicknesses of the steel frame's outer side beams W12×53 and corner columns W12×87 are worth considering for the influence of geometrical characteristics. Their expected linear regression coefficients are 1.46e-2 and 7.82e-3, with standard deviations of 2.53e-3 and 1.99e-3, respectively. Finally, the expected linear regression coefficient for the load

Table 8
Five best models of prediction.

Variable	Prob.	Expected value	Standard deviation	Model 1	Model 2	Model 3	Model 4	Model 5
Intercept	100	−2.48E-01	5.93E-01	6.44E-02	−7.67E-02	−3.57E-02	−1.38E-01	−2.35E-01
Elas_26	0.1	3.56E-10	1.62E-08	.	.	.	.	.
Elas_53	0	0.00E+00	0.00E+00	.	.	.	.	.
Elas_60	0	0.00E+00	0.00E+00	.	.	.	.	.
Elas_87B	0	0.00E+00	0.00E+00	.	.	.	.	.
Elas_87C	39	2.92E-07	4.10E-07	.	.	.	.	7.68E-07
Elas_120	0.7	1.95E-09	2.93E-08	.	.	.	.	.
Yie_26	0	0.00E+00	0.00E+00	.	.	.	.	.
Yie_53	100	1.52E-03	1.20E-04	1.52E-03	1.52E-03	1.52E-03	1.50E-03	1.52E-03
Yie_60	1.1	1.84E-06	2.27E-05	.	.	.	.	.
Yie_87B	1.4	1.88E-06	1.94E-05	.	.	.	.	.
Yie_87C	100	1.11E-03	1.35E-04	1.11E-03	1.12E-03	1.10E-03	1.12E-03	1.11E-03
Yie_120	39.3	9.57E-05	1.34E-04	.	.	.	2.50E-04	.
Hei_26	11.1	−4.01E-04	1.29E-03	.	.	.	.	.
Hei_53	14.5	3.87E-04	1.06E-03	.	.	.	.	.
Hei_60	0	0.00E+00	0.00E+00	.	.	.	.	.
Hei_87B	9	1.79E-04	6.47E-04	.	.	.	.	.
Hei_87C	0	0.00E+00	0.00E+00	.	.	.	.	.
Hei_120	0	0.00E+00	0.00E+00	.	.	.	.	.
Wid_26	0.8	1.37E-05	2.03E-04	.	.	.	.	.
Wid_53	4.8	5.68E-05	2.96E-04	.	.	.	.	.
Wid_60	0	0.00E+00	0.00E+00	.	.	.	.	.
Wid_87B	0.6	2.94E-06	5.22E-05	.	.	.	.	.
Wid_87C	2.2	2.01E-05	1.64E-04	.	.	.	.	.
Wid_120	0	0.00E+00	0.00E+00	.	.	.	.	.
Flan_26	54.9	7.62E-03	7.91E-03	.	1.36E-02	.	1.37E-02	1.43E-02
Flan_53	100	1.46E-02	2.53E-03	1.48E-02	1.49E-02	1.45E-02	1.50E-02	1.46E-02
Flan_60	32.4	1.94E-03	3.14E-03	.	.	6.40E-03	.	.
Flan_87B	35.2	1.21E-03	1.84E-03	.	.	.	.	.
Flan_87C	100	7.82E-03	1.99E-03	7.72E-03	7.89E-03	7.56E-03	7.89E-03	8.24E-03
Flan_120	23.6	5.57E-04	1.12E-03	.	.	.	.	.
Web_26	0	0.00E+00	0.00E+00	.	.	.	.	.
Web_53	0	0.00E+00	0.00E+00	.	.	.	.	.
Web_60	5.4	4.49E-04	2.16E-03	.	.	.	.	.
Web_87B	0	0.00E+00	0.00E+00	.	.	.	.	.
Web_87C	2.3	1.25E-04	9.89E-04	.	.	.	.	.
Web_120	0	0.00E+00	0.00E+00	.	.	.	.	.
Loads	100	9.27E-07	1.99E-07	9.40E-07	9.18E-07	9.31E-07	9.18E-07	9.23E-07
Number of variables				5	6	6	7	7
Determination factor (R^2)				0.219	0.224	0.224	0.229	0.229
Bayesian information criterion (BIC)				−2.13E+2	−2.13E+2	−2.12E+2	−2.12E+2	−2.12E+2
Posterior probability				0.019	0.019	0.018	0.017	0.017

factor is 9.27e-7, with a standard deviation of 1.99e-7. These numbers are exceedingly minor compared to the effects of material and geometry factors, but they should still be taken into account because they show up 100% in models that estimate steel frame resistance, especially the self-weight of construction components and accessories.

Fig. 10 depicts the occurrence probability of predictors in models that forecast the maximum load factor of the steel frame. The results demonstrate that the influence of uncertainty in elastic modulus values has negligible effect on steel frame behavior. Only the elastic modulus of W12×87 shaped steel columns is relevant since it occurs in the models at about 39% of the total. The elastic modulus of W12×26 shaped steel beams emerges in the models at only about 0.1%, whereas the rest of the members have no meaningful influence. The uncertainty of the yield stress value is notable in comparison to the elastic modulus value. The yield strength of steel beams W12×53 and steel columns W12×87 appears in the predicted models at 100%, whereas steel columns in W12×120 appear at 39.3%, upper floor steel columns W10×60, and steel beams in between W12×87 appear at 1.1% and 1.4%, respectively. The yield strength of the W12×26 transverse beams, in particular, does not show in the predicted models. For the structural cross-sectional height, the influence of the height of the W12×53 steel beams appears to be approximately 14.5%, 11.1% for the W12×26 beams, and 9% for the W12×87 beams. The rest does not appear in the models. Variation in member flange width has insignificant effect on steel frame behavior. Its occurrence in the models is predicted to be exceedingly small, approximately 4.8% for W12×53 beams, 2.2% for W12×87 columns, and the remainder is negligible. Meanwhile, flange thickness uncertainties are obvious as they feature prominently in the predicted models. The flange thickness parameters of W12×53 beams and W12×87 columns appear in the models 100% of the time, 54.9% for W12×26 beams, 32.4% for W10×60 columns, 35.2% for W12×87 beams, and 23.6% for W12×120 columns. The influence of uncertainty in web thickness of members is likewise negligible. Only steel columns W10×60 and W12×85 occur in the predicted models with probabilities of 5.4% and 2.3%, respectively. The remaining elements are nearly nonexistent.

Consequently, the results of the analysis of the multi-variable linear regression models according to the BMA method for a typical steel frame indicate that in the design of steel frame structures, the geometrical and material properties of the structures' outer boundary beams and steel columns at structural corners should be given special consideration. Inaccurate calculations to limit mistakes when assessing the self-weight of components and accessories prior to their incorporation into the design must also be addressed since they pose a danger of overestimating the structure's load-carrying capacity. In addition, it is required to pay special attention to checking the placements of these components during maintenance work in order to make an acceptable correct assessment of the steel frames' operating capacity instead of being time-consuming to check the whole components of the structure.

5. Conclusions

This study proposes a probability model, the so-called SPAAP, based

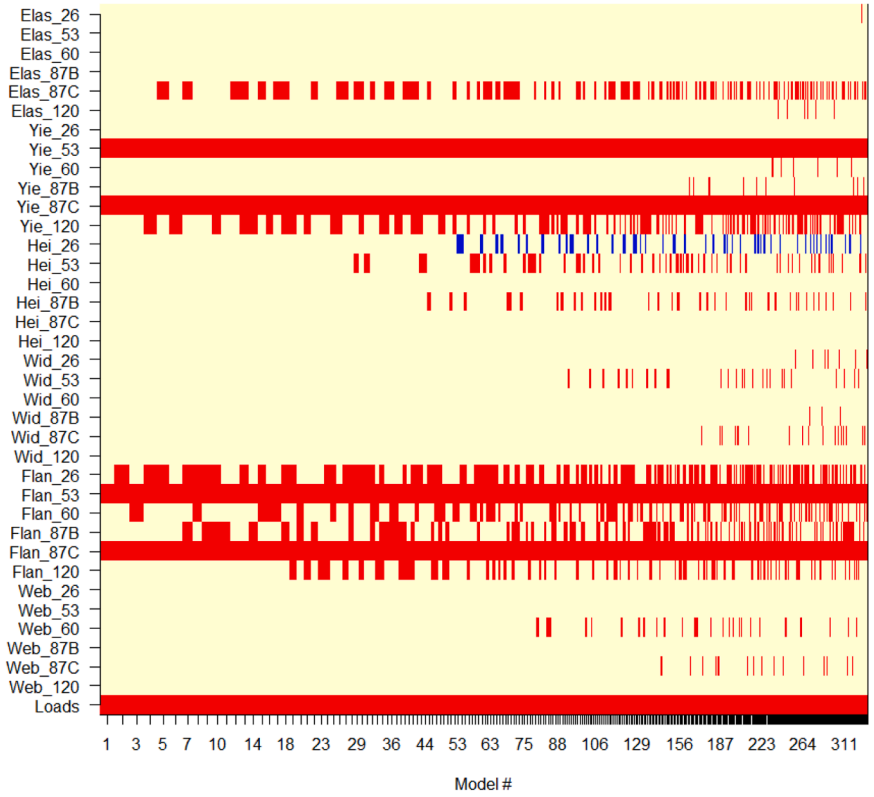

Fig. 10. Predictive models selected by BMA method. (For interpretation of the references to colour in this figure legend, the reader is referred to the web version of this article.)

on non-intrusive MCS simulation combined with advanced nonlinear inelastic analysis to generate a random set of structural steel frame responses. The statistical dataset of the stochastic response of a typical steel structure illustrated the efficiency of the proposed method. The conclusions of this study can be drawn as follows.

- The stochastic analysis of the load carrying capability of the steel frame produces more accurate results than the deterministic analysis. The findings of the stochastic analysis invariably converge to a value lower than about 3% indicating that the deterministic analysis results based on the nominal input parameters are less accurate. A stochastic analysis should be carried out during the practical design to define an appropriate safety factor instead of using the safety factor in the standards to aim at saving construction costs.
- The LHS random variable generation technique associated with a refined plastic-hinge analysis algorithm is highly successful for approximate study of steel frame behavior due to the ability of convergence after about 350 repetitions.
- The yield strength of the material has a major influence on the ultimate resistance of the steel frame. In order to increase the load-carrying capacity of the steel structure's frame, it is recommended to increase the yield strength of steel rather than other characteristic factors.
- The beam members on the sides and columns at the corners of the lower levels are extremely sensitive to the steel frame's response. Therefore, it is essential to pay careful attention to these input parameters in the computational simulation and to make better decisions regarding the maintenance of steel frame components.

CRediT authorship contribution statement

Huy-Khanh Dang: Conceptualization, Methodology, Formal analysis, Investigation, Writing – original draft, Writing – review & editing. **Duc-Kien Thai:** Investigation, Writing – review & editing. **Seung-Eock Kim:** Resources, Supervision, Writing – review & editing.

Declaration of Competing Interest

The authors declare that they have no known competing financial interests or personal relationships that could have appeared to influence the work reported in this paper.

Data availability

No data was used for the research described in the article.

Acknowledgements

This research was supported by the National Research Foundation of Korea (NRF) grant funded by the Korean government (MSIT) (No.2021R1A2B5B01002577).

References

[1] Mazzotta V, Brunesi E, Nascimbene R. Numerical modeling and seismic analysis of tall steel buildings with braced frame systems. Period Polytech Civ Eng 2017;61:196–208. https://doi.org/10.3311/PPci.9469.
[2] Fan H, Li QS, Tuan AY, Xu L. Seismic analysis of the world's tallest building. J Constr Steel Res 2009;65:1206–15. https://doi.org/10.1016/j.jcsr.2008.10.005.
[3] Truong VH, Vu QV, Thai HT, Ha MH. A robust method for safety evaluation of steel trusses using Gradient Tree Boosting algorithm. Adv Eng Softw 2020;147:102825. https://doi.org/10.1016/j.advengsoft.2020.102825.
[4] Degertekin SO, Tutar H. Optimized seismic design of planar and spatial steel frames using the hybrid learning based jaya algorithm. Adv Eng Softw 2022;171:103172. https://doi.org/10.1016/j.advengsoft.2022.103172.
[5] Yang JS, Chen JB, Beer M, Jensen H. An efficient approach for dynamic-reliability-based topology optimization of braced frame structures with probability density evolution method. Adv Eng Softw 2022;173:103196. https://doi.org/10.1016/j.advengsoft.2022.103196.

[6] Zakian P. Meta-heuristic design optimization of steel moment resisting frames subjected to natural frequency constraints. Adv Eng Softw 2019;135:102686. https://doi.org/10.1016/j.advengsoft.2019.102686.

[7] Rodríguez D, Brunesi E, Nascimbene R. Fragility and sensitivity analysis of steel frames with bolted-angle connections under progressive collapse. Eng Struct 2021; 228:111508. https://doi.org/10.1016/j.engstruct.2020.111508.

[8] Wijesundara KK, Nascimbene R, Rassati GA. Evaluation of the seismic performance of suspended zipper column concentrically braced steel frames. J Constr Steel Res 2018;150:452–61. https://doi.org/10.1016/j.jcsr.2018.09.003.

[9] Wijesundara KK, Nascimbene R, Rassati GA. Modeling of different bracing configurations in multi-storey concentrically braced frames using a fiber-beam based approach. J Constr Steel Res 2014;101:426–36. https://doi.org/10.1016/j.jcsr.2014.06.009.

[10] Kaveh A, Nasrollahi A. Performance-based seismic design of steel frames utilizing charged system search optimization. Appl Soft Comput J 2014;22:213–21. https://doi.org/10.1016/j.asoc.2014.05.012.

[11] Dinh-Cong D, Nguyen-Thoi T, Nguyen DT. A FE model updating technique based on SAP2000-OAPI and enhanced SOS algorithm for damage assessment of full-scale structures. Appl Soft Comput J 2020;89:106100. https://doi.org/10.1016/j.asoc.2020.106100.

[12] Ha MH, Vu QV, Truong VH. Optimization of nonlinear inelastic steel frames considering panel zones. Adv Eng Softw 2020;142:102771. https://doi.org/10.1016/j.advengsoft.2020.102771.

[13] Clough RW, Wilson EL. Early finite element research at berkeley. Mech: Fifth US Natl Conf Comput; 1999. p. 1–35.

[14] Alemdar BN, White DW. Displacement, Flexibility, and Mixed Beam-Column Finite Element Formulations for Distributed Plasticity Analysis. J Struct Eng 2005;131: 1811–9. https://doi.org/10.1061/(ASCE)0733-9445(2005)131.

[15] Jiang X, Chen H, Liew JYR. Spread-of-plasticity analysis of three-dimensional steel frames. J Constr Steel Res 2002;58:193–212.

[16] Teh LH, Clarke MJ. Plastic-zone analysis of 3D Steel Frames Using Beam Elaments. J Strucutral Eng 1999;125:1328–37.

[17] Nguyen PC, Kim SE. Second-order spread-of-plasticity approach for nonlinear time-history analysis of space semi-rigid steel frames. Finite Elem Anal Des 2015;105: 1–15. https://doi.org/10.1016/j.finel.2015.06.006.

[18] Rajapakse RMCM, Wijesundara KK, Nascimbene R, Bandara CS, Dissanayake R. Accounting axial-moment-shear interaction for force-based fiber modeling of RC frames. Eng Struct 2019;184:15–36. https://doi.org/10.1016/j.engstruct.2019.01.075.

[19] Liew JYR, Chen H, Shanmugam NE, Chen WF. Improved nonlinear plastic hinge analysis of space frame structures. Eng Struct 2000;22:1324–38. https://doi.org/10.1016/S0141-0296(99)00085-1.

[20] Ngo-Huu C, Nguyen PC, Kim SE. Second-order plastic-hinge analysis of space semi-rigid steel frames. Thin-Walled Struct 2012;60:98–104. https://doi.org/10.1016/j.tws.2012.06.019.

[21] Kim SE, Lee J. Improved refined plastic-hinge analysis accounting for local buckling. Eng Struct 2001;23:1031–42. https://doi.org/10.1016/S0143-974X(01)00068-2.

[22] Kim SE. Practical Advanced Analysis Software for Space Steel Structures Design. Steel Struct 2006;6:107–20.

[23] Liew JYR, White DW, Chen WF. Second-order refined plastic-hinge analysis for frame design. Part I. J Struct Eng Eng 1994;119:3196–216.

[24] Liu SW, Liu YP, Chan SL. Direct analysis by an arbitrarily-located-plastic-hinge element - Part 2: spatial analysis. J Constr Steel Res 2014;103:316–26. https://doi.org/10.1016/j.jcsr.2014.07.010.

[25] Der Kiureghian A, O Ditlevsen. Aleatory or epistemic? Does it matter? Struct Saf 2009;31:105–12. https://doi.org/10.1016/j.strusafe.2008.06.020.

[26] Melcher J, Kala Z, Holický M, Fajkus M, Rozlívka L. Design characteristics of structural steels based on statistical analysis of metallurgical products. J Constr Steel Res 2004;60:795–808. https://doi.org/10.1016/S0143-974X(03)00144-5.

[27] Bartlett FM, Jelinek JJ, Schmidt BJ, Dexter RJ, Graeser MD, Galambos TV. Updating standard shape material properties database for design and reliability. Suite 3100, Chicago, 60601-2001: Am Inst Steel Constr One East Wacker Drive; 2001. p. 168.

[28] Ellingwood BR. Reliability-based condition assessment and LRFD for existing structures. Struct Saf 1996;18:67–80. https://doi.org/10.1016/0167-4730(96)00006-9.

[29] Bulleit WM. Uncertainty in Structural Engineering. Pract Period Struct Des Constr 2008;13:24–30. https://doi.org/10.1061/(asce)1084-0680(2008)13:1(24).

[30] Nadolski V, Sykora M. Uncertainty in Resistance Models for Steel Members. Trans VŠB – Tech Univ Ostrava. Civ Eng Ser 2015;14:26–37. https://doi.org/10.2478/tvsb-2014-0028.

[31] Wang P, Li C, Liu F, Zhou H. Global sensitivity analysis of failure probability of structures with uncertainties of random variable and their distribution parameters. Eng Comput 2021. https://doi.org/10.1007/s00366-021-01484-7.

[32] Chen J, Wan Z. A compatible probabilistic framework for quantification of simultaneous aleatory and epistemic uncertainty of basic parameters of structures by synthesizing the change of measure and change of random variables. Struct Saf 2019;78:76–87. https://doi.org/10.1016/j.strusafe.2019.01.001.

[33] Trinh MC, Jun H. Stochastic bending and buckling analysis of laminated composite plates using latin hypercube sampling. London: Springer; 2021. https://doi.org/10.1007/s00366-021-01544-y.

[34] Deng Z, Guo Z. Interval identification of structural parameters using interval overlap ratio and Monte Carlo simulation. Adv Eng Softw 2018;121:120–30. https://doi.org/10.1016/j.advengsoft.2018.04.006.

[35] Bergman LA, Shinozuka M, Bucher CG, Sobczyk K, Dasgupta G, Spanos PD, et al. A state-of-the-art report on computational stochastic mechanics. Probabilistic Eng Mech 1997;12:197–321. https://doi.org/10.1016/s0266-8920(97)00003-9.

[36] Schuëller GI. Computational stochastic mechanics - Recent advances. Comput Struct 2001;79:2225–34. https://doi.org/10.1016/S0045-7949(01)00078-5.

[37] Sofi A, Romeo E, Barrera O, Cocks A. An interval finite element method for the analysis of structures with spatially varying uncertainties. Adv Eng Softw 2019; 128:1–19. https://doi.org/10.1016/j.advengsoft.2018.11.001.

[38] Roger GG, Pol DS. Stochastic finite elements - A spectral approach. ineola. New York: Dover publications, INC; 2003.

[39] Papadrakakis M, Kotsopulos A. Parallel solution methods for stochastic finite element analysis using Monte Carlo simulation. Comput Methods Appl Mech Eng 1999;168:305–20. https://doi.org/10.1016/S0045-7825(98)00147-9.

[40] Wang Z, Ghanem R. An extended polynomial chaos expansion for PDF characterization and variation with aleatory and epistemic uncertainties. Comput Methods Appl Mech Eng 2021;382:113854. https://doi.org/10.1016/j.cma.2021.113854.

[41] Thuan NV, Hien TD. Stochastic Perturbation-Based Finite Element for Free Vibration of Functionally Graded Beams with an Uncertain Elastic Modulus. Mech Compos Mater 2020;56:485–96. https://doi.org/10.1007/s11029-020-09897-z.

[42] Bogoclu C, Roos D, Nestorović T. Local Latin hypercube refinement for multi-objective design uncertainty optimization[*Formula presented*]. Appl Soft Comput 2021;112:107807. https://doi.org/10.1016/j.asoc.2021.107807.

[43] Chen WF, Lui EM. Structural stability - Theory and implementation. Elsevier Science Publishing Co.,INC; 1987.

[44] Kim SE, Park MH, Choi SH. Direct design of three-dimensional frames using practical advanced analysis. Eng Struct 2001;23:1491–502. https://doi.org/10.1016/S0141-0296(01)00041-4.

[45] Ziemian R.D. Guide to stability design criteria for metal structures. 2010.

[46] Orbison JG, McGuire W, Abel JF. Yield surface applications in nonlinear steel frame analysis. Comput Methods Appl Mech Eng 1982;33:557–73. https://doi.org/10.1016/0045-7825(82)90122-0.

[47] Kim SE, Chen WF. A sensitivity study on number of elements in refined plastic-hinge analysis. Comput Struct 1998;66:665–73. https://doi.org/10.1016/S0045-7949(97)00081-3.

[48] WF C, Kim S-E. LRFD steel design using advanced analysis. New York: CRC Press; 1997.

[49] ANSI/AISC 360-16. Specification for Structural Steel Buildings. Am Inst Steel Constr 2016:1–612.

[50] Thai HT, Kim SE. Practical advanced analysis software for nonlinear inelastic analysis of space steel structures. Adv Eng Softw 2009;40:786–97. https://doi.org/10.1016/j.advengsoft.2009.02.001.

[51] Thai HT, Kim SE, Kim J. Improved refined plastic hinge analysis accounting for local buckling and lateral-torsional buckling. Steel Compos Struct 2017;24:339–49. https://doi.org/10.12989/scs.2017.24.3.339.

[52] Kim SE, Lee J, Park JS. 3-D second-order plastic-hinge analysis accounting for lateral torsional buckling. Int J Solids Struct 2002;39:2109–28. https://doi.org/10.1016/S0143-974X(01)00068-2.

[53] Batoz J-L, Dhatt G. Incremental displacement algorithms for nonlinear problems. Int J Numer Methods Eng 1979;14:1262–7. https://doi.org/10.1002/nme.1620140811.

[54] Bin Yang Y, MS Shieh. Solution method for nonlinear problems with multiple critical points. AIAA J 1990;28:2110–6. https://doi.org/10.2514/3.10529.

[55] Tokdar ST, Kass RE. Importance sampling: a review. Wiley Interdiscip Rev Comput Stat 2010;2:54–60. https://doi.org/10.1002/wics.56.

[56] American Institute of Steel Construction. AISC steel construction manual. 13th editon 2005.

[57] Orbison JG. Nonlinear static analysis of three-dimensional steel frames. dissertation. Department of Structural Engineering, Cornell University; 1982.

[58] Nguyen PC, Kim SE. An advanced analysis method for three-dimensional steel frames with semi-rigid connections. Finite Elem Anal Des 2014;80:23–32. https://doi.org/10.1016/j.finel.2013.11.004.

[59] Sedor K. The Law of Large Numbers and its Applications. Honours Semin Lakehead Univ Canada 2015;4301:1.

[60] Lyon A. Why are normal distributions normal? Br J Philos Sci 2014;65:621–49. https://doi.org/10.1093/bjps/axs046.

[61] Nowak AS, Collins KR. Reliability of structures. McGraw-Hill; 2000.

[62] Papadrakakis M, Papadopoulos V, Lagaros ND. Structural reliability analyis of elastic-plastic structures using neural networks and Monte Carlo simulation. Comput Methods Appl Mech Eng 1996;136:145–63. https://doi.org/10.1016/0045-7825(96)01011-0.

[63] Iman RL, Conover WJ. Small sample sensitivity analysis techniques for computer models, with an application to risk assessment. Commun Stat - Theory Methods 1980;9:1749–842. https://doi.org/10.1080/03610928008827996.

[64] Novak D, Teply B, Shiraishi N. Sensitivity Analysis of Structures: a Review. Dev Comput Eng Mech 2009;19:201–7. https://doi.org/10.4203/ccp.19.8.1.

[65] Shapiro SS, Wilk MB, Chen HJ. A Comparative Study of Various Tests for Normality. Am Stat Assoc Stable 1968;63:1343–72. http://www.jstor.org/stable/2285889.

[66] Raftery AE, Madigan D, Hoeting JA. Bayesian Model Averaging for Linear Regression Models. J Am Stat Assoc 1997;92:179–91.